

Power line conductor icing prevention by the Joule effect: parametric analysis and energy requirements

Zsolt Péter, Masoud Farzaneh*, László I. Kiss

NSERC / Hydro-Québec / UQAC Industrial Chair on Atmospheric Icing of Power Network Equipment (CIGELE) and Canada Research Chair on Engineering of Power Network Atmospheric Icing (INGIVRE) at Université du Québec à Chicoutimi.
555, boulevard de l'Université, Québec, Canada, G7H 2B1, <http://cigele.ca>

Abstract—The main objective of this study is to elaborate a mathematical model to calculate the minimum current intensity needed to prevent potentially damaging ice accretion on power line conductors resulting from freezing precipitations. The influence of atmospheric parameters, namely wind speed, air temperature and liquid water content (LWC), is taken into account, and is investigated on A1/S1A conductor type, namely with code word Carillon. Knowing the atmospheric parameters, as well as the duration of the freezing conditions, it is possible to calculate the energy required to prevent ice accretion on a line conductor using the Joule effect. The mathematical model elaborated for this purpose has been compared with the experiments and simulations performed at the icing wind tunnel and climate room of the CIGELE research laboratories. In order to complete the model, it is necessary to assess the equivalent thermal conductivity of the conductor, which allows the determination of the temperature distribution in the power line conductor. The radial component of the thermal conductivity is estimated on the basis of experiments performed in the wind tunnel. The experimental results are compared with values obtained from theoretically equivalent conductivity models.

I. INTRODUCTION

It is well known that freezing precipitations are responsible for major damages incurred on a large number of exposed structures, including overhead power lines. A number of active and passive methods or techniques have been proposed or developed to answer this problem, in particular ones based on the Joule heating of line conductors. The main objective of the present work is to analyze the energy requirements of icing prevention methods based on the Joule heating technique, a so-called anti-icing method. This protection technique should be applied a certain time before and during the freezing precipitation. In the present technique, namely ice prevention by the Joule effect, the nominal current in the overhead conductor is increased to ensure a conductor temperature greater than 0 degree Celsius.

The first study on the current required to prevent ice formation on line conductors was performed by J.E. Clem in 1930 [9]. He considered that heat loss by convection was significantly greater than by radiation, so that his proposed Equation (1) only takes convection into account.

$$\Delta T = 8.18 \cdot 10^{-4} \cdot I^2 R / \sqrt{Dv} \quad (1)$$

where ΔT (°C) is the conductor temperature raise above surrounding air, I (A) is the electric current in the conductor, R (Ω/km) the conductor electrical resistance, D the conductor diameter and v (m/s) the wind velocity crosswise to the conductor. Later in 1978, McComber et al. included the heat loss due to impinging water droplets in their study [12], where the required electric current was assumed to be a function of wind velocity and LWC for smooth and stranded conductors (with cylindrical and trapezoidal strands).

Measurements about the required current as function of the liquid water content are repeated in this work. In addition, the influence of air temperature at different wind velocities is examined. Energy analysis is developed for a specific type of conductor, namely an aluminium conductor steel reinforced (ACSR) conductor with circular cylindrical wire and concentric layers. This conductor is specified as A1/S1-521 (42/7) in CSA (Canadian Standards Association) standards due to adopting the IEC (International Electrotechnical Commission) designation system [4]. The mathematical formulation is completed by wind tunnel experiments providing a good estimation of the equivalent thermal conductivity and overall heat transfer coefficient around the stranded conductor.

II. MATHEMATICAL FORMULATION

The general heat balance of the line conductor may be written as next:

$$\dot{Q}_j + \dot{Q}_f + \dot{Q}_k = \dot{Q}_c + \dot{Q}_e + \dot{Q}_w + \dot{Q}_r \quad (2)$$

where \dot{Q}_j (W) is the rate of heat generation by Joule effect, \dot{Q}_f (W) is the combined heat flow rate due to stagnation and friction effects in the boundary layer, \dot{Q}_k (W) is the kinetic energy rate of the impinging water droplets, \dot{Q}_c (W) and \dot{Q}_e (W) are the heat loss rates due to convection and evaporation respectively, \dot{Q}_w (W) is the rate of heat loss due to driving rain, \dot{Q}_r (W) is the rate of radiative heat gain and/or loss.

The terms of Equation (2) can be parameterized as follows (Equations (3) to (9)).

$$\dot{Q}_j = I^2 RL \quad (3)$$

where R (Ω/m) is the electrical resistance of the conductor per unit length, L (m) is the length of the conductor. Terms (4) and (6) are borrowed from [11].

* CIGELE/INGIVRE Chairholder

$$\dot{Q}_f = hrv^2 A' / 2c_p \quad (4)$$

where h (W/m²K) is the average heat transfer coefficient, c_p (J/kgK) the specific heat of air, r is an empirical recovery factor, and A' (m²) the fraction of the conductor surface in contact with the air superheated by stagnation and friction effects. Considering our case, the flow velocity is well below the sonic velocity, consequently this effect is practically negligible.

The contribution of kinetic energy of the water droplets, \dot{Q}_k , to the general heat balance equation is not significant on stationary objects under natural atmospheric conditions [11]. Therefore it can be neglected. The convective term is

$$\dot{Q}_c = hA(T_s - T_a) \quad (5)$$

where T_s (°C) is the conductor surface temperature, and T_a (°C) the air temperature. The term considering evaporation is

$$\dot{Q}_e = 0.62hl_e A_w (e_s - e_a) / c_p p_a \quad (6)$$

where l_e (J/kg) is the latent heat of evaporation, A_w (m²) the wetted surface of the conductor, e_s (Pa) and e_a (Pa) the saturation vapour pressures at surface and air temperature over water, respectively, and p_a (Pa) the free atmospheric pressure. The rate of heat taken away by the water droplets is

$$\dot{Q}_w = WvEDLc_w (T_s - T_a) \quad (7)$$

where W (kg/m³) is the liquid water content LWC, v (m/s) is the air velocity of the free stream, E is the collection efficiency and c_w (J/kgK) is the specific heat of liquid water. In Equation (7), the water droplet temperature is considered to be the same as that of the air. Langmuir and Blodgett offer tabulated results for the overall collection efficiency in [8]. Furthermore, a formula fitted on these results can be found in [11]. The LWC can be calculated from the precipitation rate using different correlations (such as that of Best or Marshall-Palmer) offered by the literature [6], [7]. The rate of radiative heat exchange is

$$\dot{Q}_r = iA_i + h_{rad} A (T_s - T_{rad}) \quad (8)$$

where i (W/m²) is the intensity of the incident solar radiation, A_i (m²) the irradiated surface of the conductor, T_{rad} (K) the radiation heat sink temperature of the environment, and h_{rad} (W/m²K) the radiative heat transfer coefficient, as defined by (9) [13].

$$h_{rad} = \sigma \varepsilon (T_s + T_{rad}) (T_s^2 + T_{rad}^2) \quad (9)$$

where σ is the Stefan-Boltzmann constant equal to $5.67 \cdot 10^{-8}$ W/m²K⁴, and ε is the conductor surface emissivity. Substituting (3)-(8) in the general heat balance of the conductor (2), the electrical current in the conductor can be expressed as shown below:

$$I = \left[\{ (T_s - T_a)(WvEDLc_w + hA) + 0.62hl_e A_w (e_s - e_a) / c_p p_a - iA_i + h_{rad} A (T_s - T_{rad}) - hrv^2 A' / 2c_p \} / RL \right]^{0.5} \quad (10)$$

Now, we suppose that when the conductor surface temperature (T_s) is exactly 0 °C, then the ice accretion on the conductor does not occur. Thereby, the required minimum

electrical current (I_c) can be calculated for the given atmospheric conditions by writing $T_s=0$ °C in (10). Finally, the required energy can be derived from (11).

$$E_r = I_c^2 R t \quad (11)$$

where E_r (Wh) is the required energy, I_c (A) the required minimum electrical current and t (h) the time during the unfavourable weather conditions rule.

The challenge in using (10) is to define the overall heat transfer coefficient for the stranded conductor. The literature offers a wide range of empirical correlations for airflow around smooth cylinder such as that of Zhukauskas or Hilpert-Morgan [5]. However, the overall heat transfer around the stranded conductor should be significantly higher than that proposed in the literature. Therefore, an attempt to estimate it empirically is made in the first part of the following section. Under typical accretion conditions, the incident solar radiation is not significant. Moreover, with increasing wind velocities, the role of the radiation heat transfer diminishes. In these cases the radiation term can be safely neglected.

III. EXPERIMENTAL SETUP AND PROCEDURE

The experimental part of the study has two objectives. First, the average heat transfer coefficient needs to be estimated in order to determine the heat convection around the stranded conductor. Second, experimental data on the required electric current to prevent ice accretion as a function of wind velocity, air temperature and LWC, need to be generated in order to assess the predictive power of the model.

A. Experimental Rig

An experimental rig was built using a low-voltage, high amperage transformer for heating a line conductor by passing alternating current through it. The effective current is measured with a current transformer installed in the circuit. The line conductor was installed in the test section of a refrigerated wind tunnel, perpendicular to the direction of the airflow. The cross-sectional dimensions of the wind tunnel test section are 18"x36". The velocity field in the wind tunnel section under study was simulated for different free stream velocities. Figure 1 shows one of the results of the computations with the wind velocity distribution in a horizontal plane.

The water droplets are injected into the refrigerated air stream by three nozzles. The distance between the spray bar, where the nozzles are fixed and the conductor is about 4.5 m. The pressures of the air and water lines are adjusted using the results presented in [1]-[3].

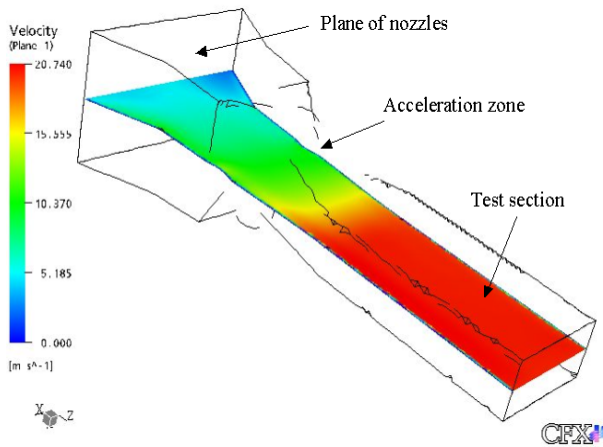


Fig. 1. Airflow simulation of wind tunnel section (between spray bar and end of test section) using a commercial CFD software (CFX-5.6). The velocity distribution is not uniform in the spray bar section.

The conductor used in the experiment was a Carillon, A1/S1-548 (42/7) conductor type, whose outside consists of 42 aluminium wires, with a core made of 7 steel wires. Its outer diameter is 30.5 mm, the length of the heated section is 850 mm, and its “surface” layer is made of 20 4-mm strands. One of these strands is hosting a thermocouple at its center (see Fig. 2). The thermocouple measuring the stagnation temperature was installed inside one of the outside strands in the middle of the test section of the conductor. Two other thermocouples were installed; one to monitor the air temperature in the wind tunnel, and another one to measure the room temperature near the conductor connections. The conductor connections are outside of the wind tunnel, in the thermally isolated room that surrounds the test section. All thermocouples were previously calibrated in crushed ice made from de-ionized water.

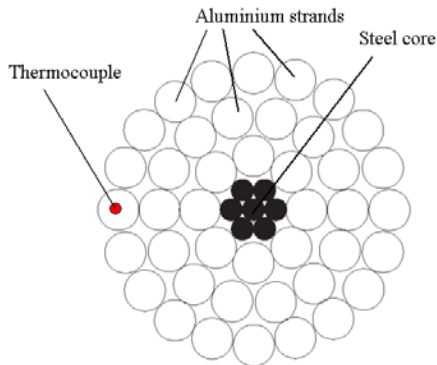


Fig. 2. Cross-sectional view of Carillon type conductor. A thermocouple is installed in the stagnation point.

It is important for the conductor to be well connected for as if the contacts between the conductor and the connector clamps are not satisfying, additional heat sources will be created, affecting the experimental results. The ends of the conductor were welded and machined to a cylindrical shape in order to increase the contact surface between the conductor and the connectors as much as possible. The connecting clamps were pressed against the conductor ends with four-four screws

tightened as much as possible to ensure a good contact. The voltage drop between the clamps at the ends indicates the goodness of the contact. The surface temperature distribution along the length of the conductor and at the connections was monitored by an infrared camera. From the images taken, it was possible to estimate the strength of the parasite heating and its effect at the middle-section of the conductor, where the thermocouple was placed. As a result, no significant parasite heat generation was found at the conductor ends. Unfortunately, few strands in the outer layer lost the tension during the conductor preparation so they have poorer contact with the other strands. Furthermore, they have greater surface exposed to airflow. Consequently ice formed on these strands before the thermocouple inside the conductor showed 0 °C.



Fig. 3. The test section of the line conductor installed in the wind tunnel.

B. Experimental procedure

Two series of tests were performed: 1.) Determining the heat convection term, 2.) Analyzing the required minimum electrical current. In the last series, the difference between the influence of the air temperature and that of the LWC was analyzed. Both series used the same experimental rig. In both cases the appropriate wind speed was adjusted by controlling the fan speed. The wind speed is measured using a hand held anemometer. The test section of the wind tunnel is a well-insulated space where the temperature is kept approximately the same as that in the wind tunnel. Therefore, the radiation heat loss from the conductor to its surrounding becomes negligible. The LWC and medium volume diameter (MVD) data are obtained from [1]-[3] for the corresponding water and air pressure settings in the nozzles.

1) Estimating the Average Convection Coefficient

The estimation of the average convection heat transfer coefficient of the stranded conductor is based on the heat balance of the electrically heated conductor under steady state, dry airflow conditions.

$$I^2 \cdot R \cdot L = h \cdot A_c \cdot (T_s - T_{air}) \quad (12)$$

The convection coefficient is calculated from Equation (12) after both the conductor surface and air temperatures are measured with a constant current in the conductor. This is repeated under different wind velocities in the range of 5 to 28 m/s. During these series, the air temperature was maintained around -10°C, as can be seen in Fig. 4. The air and the conductor surface temperatures in the wind tunnel were continuously registered (see Fig. 4) and the average values of the steady state period were computed.

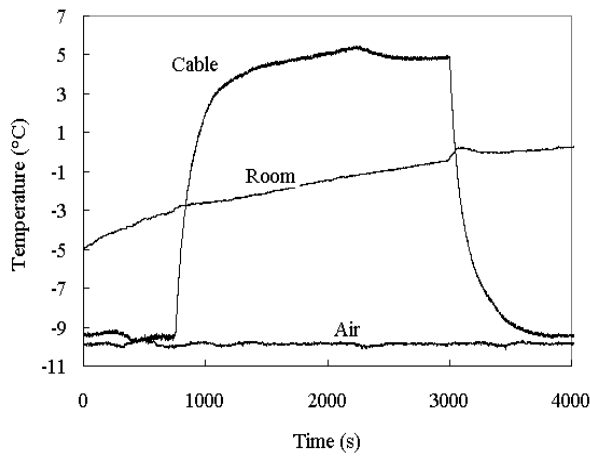


Fig. 4. Registered temperature history during a typical test. $I=1900$ A, airflow velocity 10 m/s.

2) Estimating the Heat Loss due to Driving Rain

The challenge with these measurements is to determine the minimum required current that prevents ice formation on the conductor section. The minimum effective current is defined by the value when the thermocouple installed in the outer layer strand reads 0°C in steady state. For this purpose the conductor and air temperatures must be continuously registered (see Fig. 5).

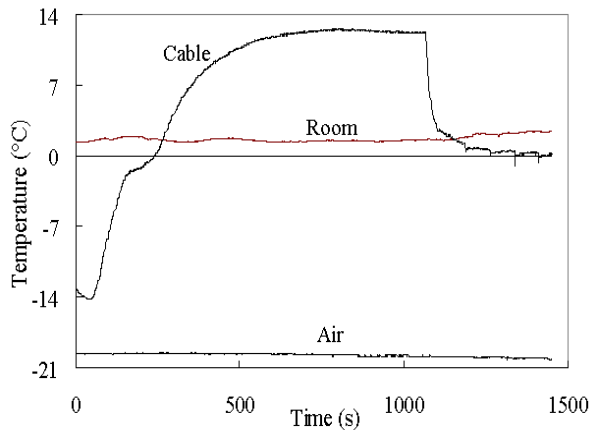


Fig. 5. Temperature history of the conductor at 10 m/s wind speed, in range of air temperature $-19.6^\circ\text{C} < T_a < -20.3^\circ\text{C}$. $LWC=5.26$ g/m³.

First, the conductor was heated from 7 to 20°C under different wind speeds, in such a manner that after being impinged by water droplets, its temperature would not fall below 0°C . When water droplets hit the conductor, its surface temperature will decrease significantly until it reaches a new steady state. Then the electric current can be decreased lightly as it is shown in Fig. 5. Unfortunately, during the tests water droplets reach the fan of the wind tunnel and after a certain time, ice accumulates on the fan blades causing air velocity drop. The air velocity is readjusted every 10 minutes in order to keep the wind speed constant with a precision of ± 0.2 m/s. Finally, we found that such small variations in the wind speed have no significant influence on the minimum current measurements.

IV. PRELIMINARY EXPERIMENTAL RESULTS

A. Convective Heat Transfer Coefficient

The convective heat transfer coefficient in the stagnation point can be estimated from (12). We will use it as an average value around the stranded conductor. Its value was measured for different wind velocities and the corresponding Nusselt numbers (Nu) were calculated. The results are presented in a general form in Fig. 6. It is clear from Fig. 6 that the Nu numbers are almost linearly related to the Re number. Therefore, Equation (13) below can be used to estimate the average heat transfer coefficient for stranded conductors in the Reynolds number range from 10^4 to $6 \cdot 10^4$.

$$Nu = 0.0076 \cdot Re \quad (13)$$

The difference between the convective heat transfer coefficient for smooth cylinder and that for a stranded conductor increases with increasing air speed.

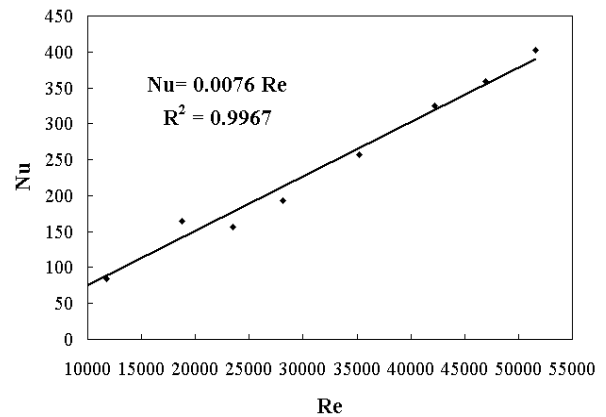


Fig. 6. Nusselt number as a function of Reynolds number. Measured for Carillon type stranded conductor.

B. Required Minimum Current

Figure 7 shows the current intensity required to prevent ice formation on the conductor as a function of LWC of air for different wind velocities. Obviously, the required current increases both with wind speed and with LWC. It can also be seen that the wind speed has a stronger influence than LWC.

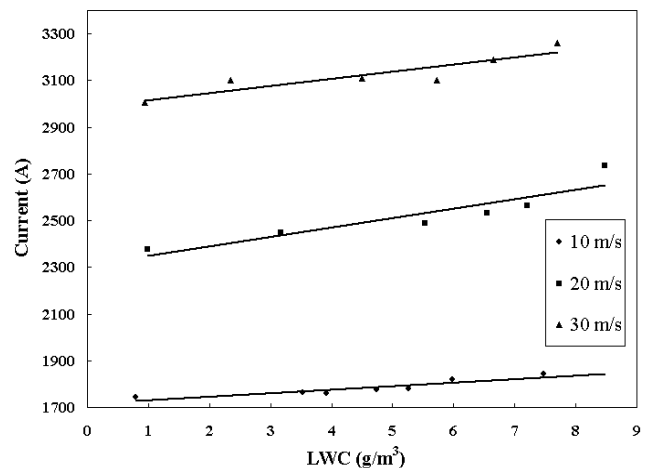


Fig. 7. Required electric current to prevent ice formation versus LWC of air, in range of air temperature $-9.4^\circ\text{C} < T_a < -9.7^\circ\text{C}$. The 30 m/s series comprises wind velocities in range $28.6 < v < 29.4$ m/s.

The required electric current as a function of air temperature

for different wind speed values is presented in Figure 8. The series with 20 m/s approaches the best the theoretical calculations by using (10). This can be seen from the comparison of Fig. 8 and Fig.10. The 10 m/s series shows higher rate of increase, while the 30 m/s series has a lower rate with increasing air temperature than those supplied by the theoretical calculations.

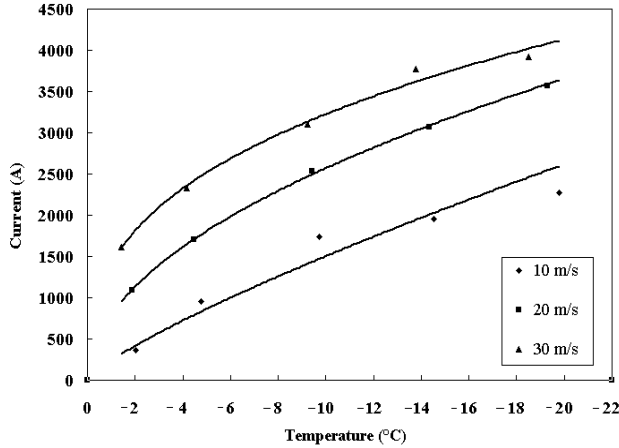


Fig. 8. Required electric current to prevent ice formation versus air temperature. The 30 m/s series comprises air velocities in range $29.1 < v < 29.4$ m/s. The LWC is 5.26 g/m^3 at 10 m/s, 6.54 g/m^3 at 20 m/s and 5.72 g/m^3 at 30 m/s wind velocity.

V. COMPARISON OF THE RESULTS

The calculations were made by using Equation (10), without the radiation term. Moreover, some of these calculations were performed without considering the problem of estimating the water evaporation of the wetted surface of the conductor. In cases when the evaporation was taken into account, the wetted surface was estimated as half of the conductor surface. In Figs. 9 and 10, different cases calculated by using the mathematical model and the corresponding experimental results are compared.

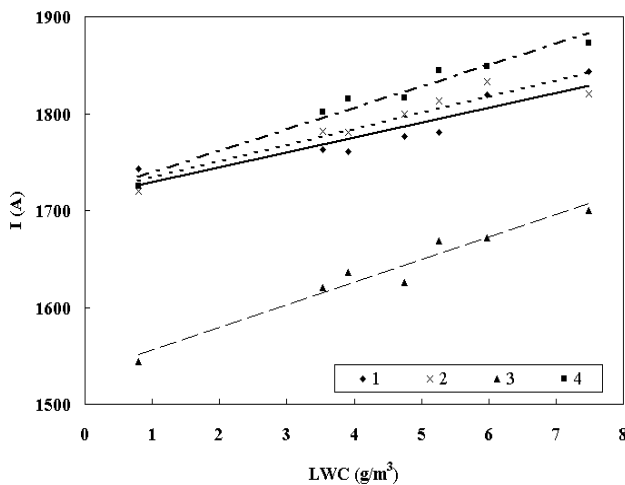


Fig. 9. Required electric current to prevent ice formation versus LWC for cases of 1. experimental result, 2. using (10) case without radiation term, 3. using (10) neglecting the radiation and evaporation terms, 4. same as 3. with constant collection coefficient, $E=0.8$. Air temperature in the range $-8.9^\circ\text{C} < T_a < -9.76^\circ\text{C}$, airflow velocity 10 m/s, MVD of droplets in range of $35\mu\text{m} < \text{MVD} < 62\mu\text{m}$.

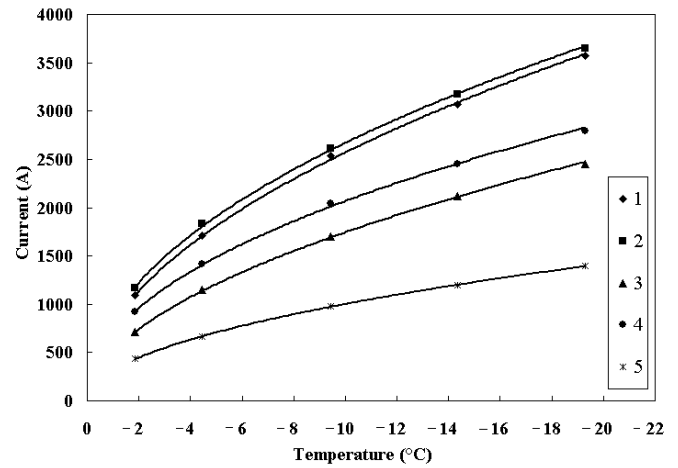


Fig. 10. Required electric current to prevent ice formation as a function of air temperature, for the following cases: 1. experimental result, 2. using (10) without radiation term considering constant collection coefficient, $E=0.8$, 3. same as 2. but without evaporation term, 4. using (10) without radiation term, with the average heat transfer coefficient is calculated using the Zhukauskas approximation for smooth cylinders, 5. using equation of Clem (1). $LWC=6.54 \text{ g/m}^3$ and airflow velocity 20 m/s.

The surface of the stranded conductor was not covered completely by a continuous water film. However, analyzing the results in Fig. 9 and Fig. 10 it can be clearly seen that the influence of water evaporation is not negligible.

VI. EQUIVALENT THERMAL CONDUCTIVITY

The previous equations included the conductor surface temperature only. The temperature distribution inside a cylindrical conductor with thermal energy generation is expressed by Equation (14).

$$T(r) = T_s + \frac{q}{4k}(r_s^2 - r^2) + \frac{q}{2k}r_c^2 \ln \frac{r}{r_s} \quad (14)$$

where $T(r)$ is the in-conductor temperature ($^\circ\text{C}$) at radius r , q (W/m^3) the volumetric heat source, r_s (m) the conductor surface radius, r_c (m) the steel core radius and k (W/mK) the thermal conductivity. The thermal conductivity of pure solid aluminium is 237 W/mK [5]. The ACSR conductor contains both aluminium and steel strands (Fig. 2), with air gaps between the circular strands. Due to its heterogeneous structure, heat conduction analysis for this conductor is more complex than if it were homogeneous. Air gaps hinder heat conduction, while contact surfaces between strands increase thermal resistance. However, this problem can be dealt simply by introducing a new transport coefficient (Fig. 11), which is called the equivalent thermal conductivity. It is interesting to notice that it is also known as “apparent”, “resultant” or “effective” conductivity in the literature [10].

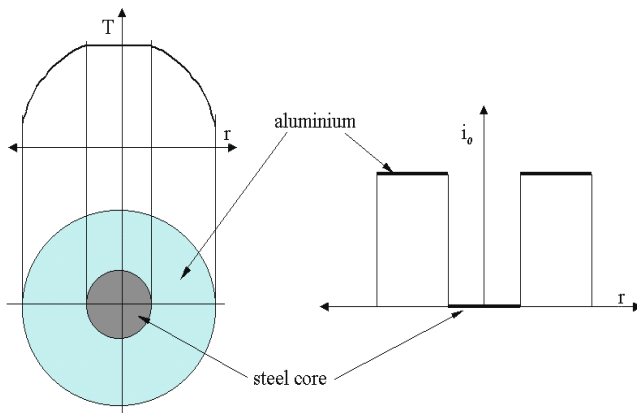


Fig. 11. Apparent temperature distribution in conductor, in case of uniform electrical current distribution in the aluminium strands without AC current in the steel core.

It was necessary to perform tests to obtain a good estimation of the equivalent thermal conductivity of the conductor. The test consists the Joule heating of the conductor with a known current intensity. Following this, the equivalent thermal conductivity can be estimated by measuring the temperature at two different points along the cross-section of the conductor at steady state. The experimental results were evaluated for two cases: i) Uniform heat generation in the conductor, ii) Considering the skin effect. The average results in both cases are presented in Table I.

TABLE I
EQUIVALENT THERMAL CONDUCTIVITY VALUES OBTAINED BY DIFFERENT METHODS FOR BERSIMIS CONDUCTOR

Method	Equivalent thermal conductivity (W/mK)
Experimental, Skin effect considered	7.0
Experimental, With uniform heat generation	7.2
Theoretical, Riemann model	8.7
Theoretical, Zehner-Bauer-Schlünder model	10.0

The relevant literature [10] offers certain theoretical models for estimating the equivalent thermal conductivity. Some of these models such as the Riemann or Zehner-Bauer-Schlünder model are adapted to the heat conduction in the aluminium strands (see Table I).

As seen from Table I, both the experimental and theoretical results are in the range of $7 < k_e < 10$ W/mK, which is an order of magnitude lower than that of the solid aluminium. This means that the contact thermal resistance between the strands plays a very important role in the radial heat conduction for this type of conductor.

VII. CONCLUSIONS

1. An experimental study was presented for analyzing the minimum electric current required to prevent ice formation on overhead conductors. The experimental results are compared with the mathematical model previsions for different cases.
2. The convective heat transfer coefficients around stranded conductors are higher than around smooth cylinders.
3. The mathematical calculations using (10) without the radiation term slightly overestimate the wind tunnel measurements due to difficulties in estimating the wetted surface and the overall convection heat transfer coefficient around a stranded conductor.
4. The equivalent thermal conductivity for stranded conductors is in the range of $7 < k_e < 10$ W/mK.

VIII. ACKNOWLEDGMENT

This work was carried out within the framework of the NSERC /Hydro-Québec/ UQAC Industrial Chair on Atmospheric Icing of Power Network Equipment (CIGELE) and Canada Research Chair on Engineering of Power Network Atmospheric Icing (INGIVRE) at the Université du Québec à Chicoutimi. The authors would like to thank all the sponsors for their financial support. We are also most grateful to Dr. Anatolij Karev and Dr. László Kollár for useful discussions.

IX. REFERENCES

- [1] A. R. Karev and M. Farzaneh, "Evolution of droplet size distribution in an icing wind tunnel," in 10th IWAIS, Brno, Czech Republic, 2002.
- [2] A. R. Karev, M. Farzaneh and M. Mousavi, "Influence of non-uniformity of droplet size distribution on ice accretion," presented at the 10th IWAIS, Brno, Czech Republic, 2002.
- [3] A. R. Karev, M. Farzaneh and L. Kollár, "An icing wind study on characteristic of an artificial aerosol cloud. Part I: Cloud uniformity and accompanying droplet size distribution," submitted to Journal of Applied Meteorology.
- [4] Alcan Cable, "Bare Overhead Cable," Canadian Product Catalogue. [Online]. Available: <http://www.cable.alcan.com>
- [5] F. P. Incropera, David P. DeWitt: Heat and Mass Transfer, 5th ed. John Wiley & Sons, pp. 410-412, 905, 2002.
- [6] G. Fortin, "Thermodynamique de la glace atmosphérique", Lecture notes, Université du Québec à Chicoutimi, 2002.
- [7] G. Poots, "Ice and Snow Accretion on Structures", Research Studies Press, pp. 15-16, 1996.
- [8] I. Langmuir, K.B. Blodgett, "A mathematical investigation of water droplet trajectories," Technical report, 5418,USAAF, pp.65.
- [9] J. E. Clem, "Currents Required to Remove Conductor Sleet," *Electrical World*, pp. 1053-1057, Dec. 1930.
- [10] L. I. Kiss, "Thermo-physical properties in heat conduction," Lecture notes, Université de Liège, LTAS, 1996.
- [11] L. Makkonen, "Estimating intensity of atmospheric ice accretion on stationary structures," *Journal of Applied Meteorology*, vol. 20, pp.595-600, May. 1981.
- [12] P. McComber, D. D. Nguyen, et J. Druetz, "Prévention par chauffage de la formation de givre de verglas sur les conducteurs cylindriques ou toronnés," *Recherche Canadienne en Génie Mécanique*, vol. 3, pp. 27-33, 1978.
- [13] Y. A. Çengel: Heat transfer: a practical approach. 2nd ed. New York: McGraw-Hill, 2003, pp. 130, 737, 868.